J Solid State Electrochem (2012) 16:2837–2843
DOI 10.1007/s10008-012-1710-y

ORIGINAL PAPER

Electrochemical determination of nonylphenol based on ionic liquid-functionalized graphene nanosheet modified glassy carbon electrode and its interaction with DNA

Xiaomeng Meng · Huanshun Yin · Minrong Xu · Shiyun Ai · Jianying Zhu

Received: 20 November 2011 / Revised: 18 February 2012 / Accepted: 27 February 2012 / Published online: 17 March 2012

Abstract Nonylphenol (NP) was determined using electrochemical method based on ionic liquid-functionalized graphene nanosheet modified electrode. The fabricated electrode was characterized by electrochemical impedance spectroscopy. The different influence parameters, such as pH value, scan rate, accumulation potential, and time, were investigated. Under the optimum conditions, the linear relationship between peak current value and concentration of NP was obtained with differential pulse voltammetry in two ranges from 0.5 to 30 μM and 30 to 200 μM with the detection limit of 0.058 μM (S/N=3). Moreover, this modified electrode was applied to NP determination in water and soil samples with the recoveries from 94.8 to 104 %, which showed the method could be applied to determine NP in environment. In addition, to explore the damage to DNA, the interaction between NP and DNA was investigated with the association constant (β) of 0.4867 and the Hill coefficient (m) of 3.75×10^5 M^{-1}, respectively.

Keywords Nonylphenol · Ionic liquid-functionalized graphene nanonsheet · Electrochemical determination · Interaction · DNA

Introduction

Nonylphenol (NP), as a toxic xenobiotic compound classified as endocrine disrupter [1], is the main biodegradation of nonylphenol ethoxylates which are used extensively as industrial surfactants. Due to its high hydrophobicity and low degradation rates, NP shows a persistent condition in soil and sewage sludge [2]. NP has received a great deal of attention in environmental protection because of the toxicity to the estrogen with the nonyl chain structure [3]. Some reports illustrated that NP had carcinogenic and histopathological effects on many organisms, such as aquatic hyphomycetes [4], freshwater organisms [5], male silver carp [6], and rosy harb [7]. Yao et al. presented that NP would induce apoptosis of Jurkat cells by a caspase-8 dependent mechanism [8]. The use of NP and its ethoxylates was prohibited by the European Directive no. 2003/53/EC in the European Union due to their toxicity [9]. Therefore, an efficient system to determine NP is required.

Until now, there are many methods for NP determination, such as fluorescence [10], ultraviolet-visible spectroscopy [11], enzyme immunoassay [12], biosorption [13], high performance liquid chromatography–fluorescence detector (HPLC-FLD) [14], and gas chromatography–mass spectrometer method [15]. Although these methods have low detection limit and high sensitivity, there are many disadvantages, such as time-intensive, expensive instruments, laborious treatment, and professional operator [16]. Recently, electrochemical methods have received increasing attention due to advantages of fast response, good sensitivity, low cost, simple operation, time-saving, and excellent selectivity. Few studies about electrochemical determination of NP were reported because it is hard to be oxidated. Therefore, a novel and effective material for improving catalytic ability was needed.

Graphene nanosheet, an atom-thick graphite, was the thinnest known material ever measured up to date [17]. As one of the carbon-based nanomaterials, graphene nanosheet possesses lower cost, larger surface area, better thermal conductivity, and special nanosheet structure than carbon

Electronic supplementary material The online version of this article (doi:10.1007/s10008-012-1710-y) contains supplementary material, which is available to authorized users.

X. Meng · H. Yin · M. Xu · S. Ai (✉) · J. Zhu
College of Chemistry and Material Science, Shandong Agricultural University,
Taian, Shandong 271018, China
e-mail: ashy@sdau.edu.cn

nanotubes [18, 19]. In recent years, graphene nanosheet has been applied in wide-ranging and diversified technological fields due to its unique physical, chemical, and mechanical properties [17, 20, 21]. Moreover, graphene nanosheet has been used as the electrode material due to its properties of promoting electron transfer reactions, large surface, excellent conductivity, and super catalytic activity, which provide a new way to develop novel biosensors and electrochemical sensors [22–25]. Wu et al. developed a sensitive biosensor based on graphene nanosheet to analyze the organophosphate pesticide [26]. Chlorpromazine was successfully determined by using graphene paste electrode with low detection limit [27]. In addition, we also determined 4-aminophenol [28], catechol, resorcinol, and hydroquinone [29] with graphene–chitosan composite film modified glassy carbon electrode.

Ionic liquid (ILs) has attracted much attention in the fields of electrochemical sensors fabrication due to its specific properties such as negligible vapor pressure, wide electrochemical windows, and good solubility [30–32]. Many materials were prepared using ILs as template solvents and exhibited large surface areas and good electrocatalytic performance [33, 34]. Besides, ILs proposed a green way to synthesize graphene nanosheet and showed a relatively high conductivity in electrochemistry [35, 36]. Ionic liquid-functionalized graphene nanosheet ($FGNS^{IL}$)-based electrochemical sensors have been reported for the detection of many compounds such as hydrogen peroxide [35], dopamine, guanine and adenine [36], NADH, and ethanol [37]. Nevertheless, to the best of our knowledge, electrochemical determination of NP using $FGNS^{IL}$ modified glassy carbon electrode has not yet been reported.

In this work, an electrochemical sensor based on ($FGNS^{IL}$) modified glassy carbon electrode for determination of NP was developed. Due to the catalytic ability of $FGNS^{IL}$, the oxidation peak current increased and the peak potential of NP decreased based on modified electrode. Moreover, the effect factors were investigated and the optimum conditions were chosen. Besides, the interaction between NP and DNA was discussed.

Experimental

Reagents and apparatus

NP was purchased from Aladdin Reagent Co. Ltd (Shanghai, China). The stock solution (1.0×10^{-2} M) of NP was prepared with anhydrous ethanol and stored in darkness at 4 °C. Herring sperm DNA was supplied by Shanghai solarbic Bioscience & Technology Co. Ltd (Shanghai, China). Ionic liquid (1-butyl-3-methylimidazolium hexafluorphosphate) was provided by Cheng Jie Chemical Co. Ltd (Shanghai, China). A high-purity graphite rod was purchased from Qingdao Duratight Carbon Co. Ltd (Qingdao, China). Other reagents were of analytical grade and used without any further purification. Phosphate buffer solution (PBS) was prepared by mixing stock solutions of 0.1 M NaH_2PO_4 and 0.1 M Na_2HPO_4 and the pH was adjusted with 0.1 M H_3PO_4 or 0.1 M NaOH.

Cyclic voltammetry and differential pulse voltammetry (DPV) were performed with CHI832A electrochemical workstation (Shanghai Chenhua Co., China). Electrochemical impedance spectroscopy was obtained using CHI660C electrochemical workstation (Shanghai Chenhua Co., China). The experiment was performed with a conventional three-electrode cell which comprised a bare glassy carbon electrode (GCE) (d=3 mm) or a modified GCE as working electrode, a saturated calomel electrode as the reference electrode, and a platinum wire as the auxiliary electrode. Transmission electron microscope (TEM) was conducted at Hitachi S-3000 N instrument (Japan).

Preparation of $FGNS^{IL}$/GCE

The pure graphene (PG) and $FGNS^{IL}$ was synthesized according to the previous reports [38, 39], respectively. The $FGNS^{IL}$ was prepared as follows: two graphite rods were inserted into IL/water with static potentials of 10 to 20 V. After 3 h of electrolysis, a black precipitate was taken out from the bottom of the reactor. The precipitate was thoroughly washed with absolute ethanol and redistilled deionized water, respectively, then dried at 60 °C in oven for 2 h. The obtained product was named as $FGNS^{IL}$. $FGNS^{IL}$ solution (0.5 mg mL^{-1}) was prepared with redistilled deionized water and dispersed sufficiently for 20 min in an ultrasound bath.

Before modification, the bare GCE was first polished clearly with 0.3 and 0.05 μm alumina slurry on chamois cloth, then cleaned by ultrasound in absolute ethanol and redistilled deionized water for 3 min, respectively, and lately dried in air before use. Then $FGNS^{IL}$ suspension was deposited on the surface of GCE and dried in the air. The modified electrode was noted as $FGNS^{IL}$/GCE and stored at 4 °C in a refrigerator when not in use.

Experimental procedure

After a certain volume of NP stock solutions and 10 mL of 0.1 M PBS were added into an electrochemical cell, the three-electrode system was installed. NP determination was carried out using DPV with 350 s accumulation at −0.2 V. DPV was recorded from 0.2 to 0.8 V with the parameters as follows: pulse amplitude, 50 mV; pulse width, 50 ms; and quiet time, 2 s. The water sample analysis was investigated with the same procedure of DPV. In addition, different concentrations of NP (10 to 50 μM) were mixed with a volume of DNA solutions, and the interaction was discussed by DPV.

Results and discussion

Characterization of FGNS^{IL}

The surface morphology of FGNS^{IL} was characterized by TEM. As shown in Fig. 1, the image of FGNS^{IL} clearly presented the transparent and wrinkled flake-like shape, which was good for maintaining a high surface area on the electrode.

Characterization of electrochemical behavior of FGNS^{IL}/GCE

In order to characterize the modified electrode, the AC impedance was carried out. Figure 2 presented the Nyquist diagrams of GCE (a) and FGNS^{IL}/GCE (b) in 5 mM $[Fe(CN)_6]^{3-/4-}$ solution containing 0.1 M KCl. As can be seen, a large semicircle in the high frequency was exhibited at the bare electrode (curve a), indicating a resistance into the electrode/solution system. Whereas, the FGNS^{IL}/GCE (curve b) showed almost a straight line, indicating a small interface electron resistance, which proved the excellent electroconductivity of FGNS^{IL}. This phenomenon suggested that FGNS^{IL} was successfully immobilized on the GCE surface.

Cyclic voltammetric behaviors of NP

To test the catalytic behavior of FGNS^{IL}, cyclic voltammograms at different electrodes were recorded in the absence (a, c) and presence (b, d, e) of 0.1 mM NP at 100 mV s^{-1}, and the results were shown in Fig. 3. No oxidation peak was obtained at FGNS^{IL}/GCE (curve c) and GCE (curve a) without NP, which indicated that FGNS^{IL} film was electroinactive in the selected potential range. When 0.1 mM NP was added into PBS, an obvious oxidation peak was observed at FGNS^{IL}/GCE (curve e), and in PG/GCE (curve d), no corresponding reduction peak was observed, which suggested that the response of NP was a typical of totally irreversible electrode reaction. Compared with the bare electrode (curve b), the oxidation peak current obtained at modified electrodes increased significantly, and the peak potential shifted negatively, which can be attributed to the excellent electron transfer ability, large surface, and good catalytic activity of PG and FGNS^{IL}. However, the FGNS^{IL}/GCE (curve e) showed a bigger peak current at lower potential to NP than that of PG/GCE (curve d), which illustrated that FGNS^{IL} had better sensitivity and was suitable for the determination of NP.

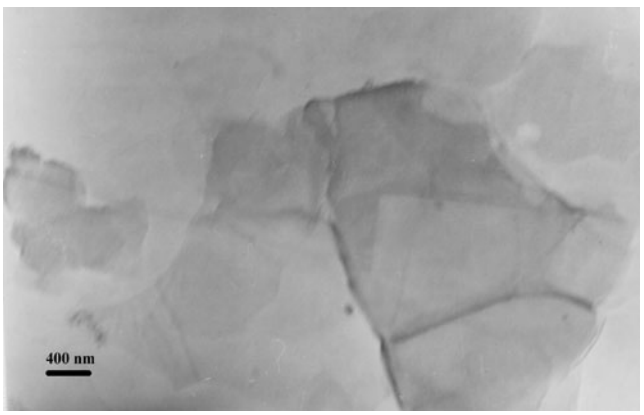

Fig. 1 The TEM of FGNS^{IL}

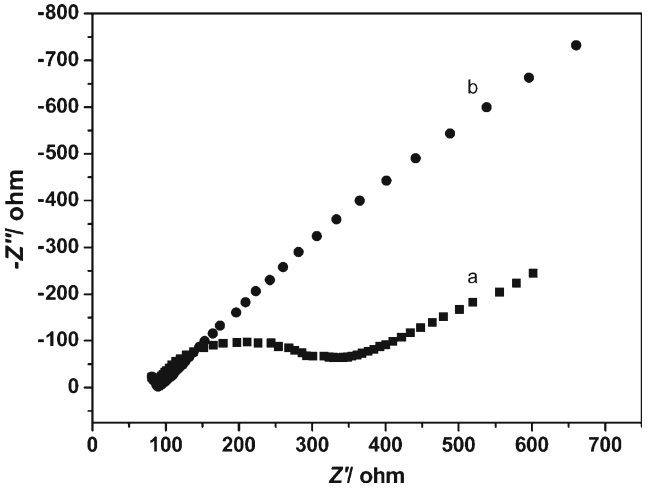

Fig. 2 Nyquist plots of GCE (*a*) and FGNS^{IL}/GCE (*b*) in 5 mM $Fe(CN)_6^{3-/4-}$ solutions containing 0.1 M KCl. Scan rate, 100 mV s^{-1}. The frequency range was from 10^{-1} to 10^5 Hz at the formal potential of 0.2 V

Optimum conditions of the modified electrode

In order to optimize the response of NP at FGNS^{IL}/GCE, the pH of supporting electrolyte was investigated over the range from 4.0 to 10.0 (Fig. 4). The oxidation peak current increased rapidly with increasing pH from 4.0 to 7.0. Then, it decreased when the pH value exceeded 8.0. In brief, the highest peak current was obtained at pH 7.0. Therefore, pH 7.0 was chosen for the subsequent experiments. As can be seen from the relationship between E_{pa} and pH, the potential decreased with the increase of pH. Moreover, it obeyed the following equation: E_{pa} (in volts)=−0.064 pH+1.026 (R=0.9949). A slope of 0.064 V pH^{-1} indicated that the numbers of electron and proton were equal in the electrode reaction [40].

As shown in Fig. 5, the effect of scan rate on voltammetric behaviors of NP was discussed, and a linear relationship of anodic peak current versus scan rate was obtained over the range from 20 to 450 mV s^{-1} with the linear regression equation of E_{pa} (in volts)=2.0023×10^{-4} v (in millivolts per second)+0.5665 (R=0.9919) (insert of

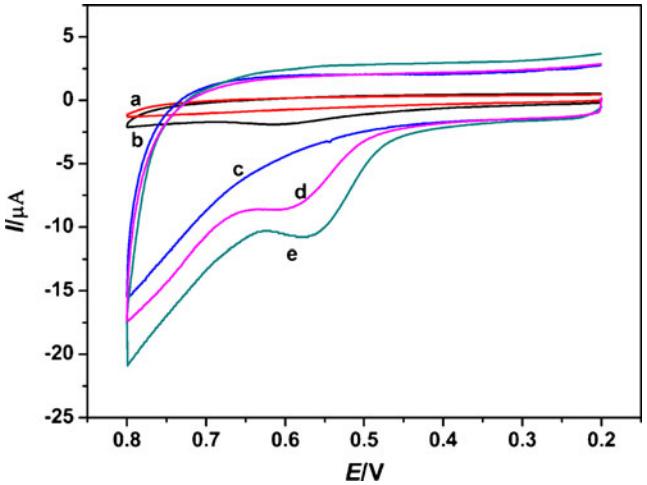

Fig. 3 Cyclic voltammograms of the bare GCE (*a*, *b*), FGNS^{IL}/GCE (*c*, *e*) and PG/GCE (*d*) in the absence (*a*, *c*) and presence (*b*, *d*, *e*) of 0.1 mM NP in 0.1 M PBS. Scan rate, 100 mV s^{-1}

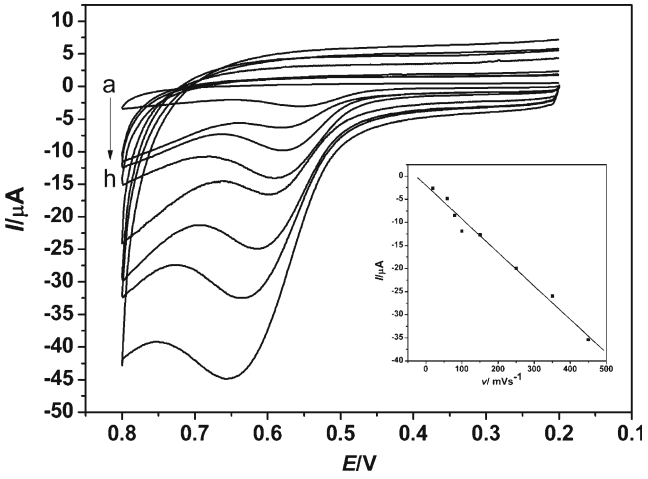

Fig. 5 Effects of scan rate on the oxidation response of 0.1 mM NP. Curves (*a*→*h*) were obtained at 20, 60, 80, 100, 150, 250, 350, 450 mV s^{-1}, respectively. *Insert* the relationship between the peak current and scan rate

Fig. 5), which indicated that the reaction of NP on FGNS^{IL}/GCE was mainly controlled by adsorption process.

The effects of accumulation potential and accumulation time were further investigated. The peak current increased rapidly when the accumulation potential shifted from 0.3 to −0.2 V. Nevertheless, it slowly decreased under more negative accumulation potential. Thus −0.2 V was selected as the optimum accumulation potential. The suitable accumulation time under the potential of −0.2 V was discussed as usual. The peak current increased with the increase of accumulation time. However, the current increased slightly when the time was longer than 350 s, which would be explained as the saturated adsorption of NP at GCE surface. Considering the efficiency and sensitivity for NP determination, 350 s was chosen as the optimum accumulation time.

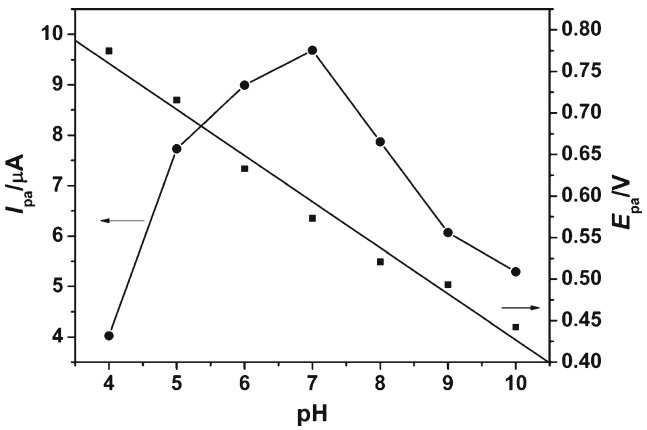

Fig. 4 Effects of pH on the current response and potential response of 0.1 mM NP on FGNS^{IL}/GCE with different pH range from 4.0 to 10.0

Calibration curve

DPV was chosen for NP detection due to its high sensitivity. Figure 6 showed the DPV curves of different concentrations of NP. As can be seen in the insert of Fig. 6, the oxidation peak current was proportional to NP concentration in the range of 0.5 to 30 μM and 30 to 200 μM under the optimum condition with the linear equations of *I* (in microamperes)=0.380 *c* (in micromolars)+0.080 (*R*=0.9993) and *I* (in microamperes)= 0.071 *c* (in micromolars)+7.024 (*R*=0.9991), respectively. The detection limit was estimated to be 0.058 μM (*S/N*=3), which was lower than the results obtained at surface plasmon resonance biosensor (7.49 μM) [41] and T/pTH/GCME (10 μM) [42]. Hence, it suggested that the FGNS^{IL} exhibited

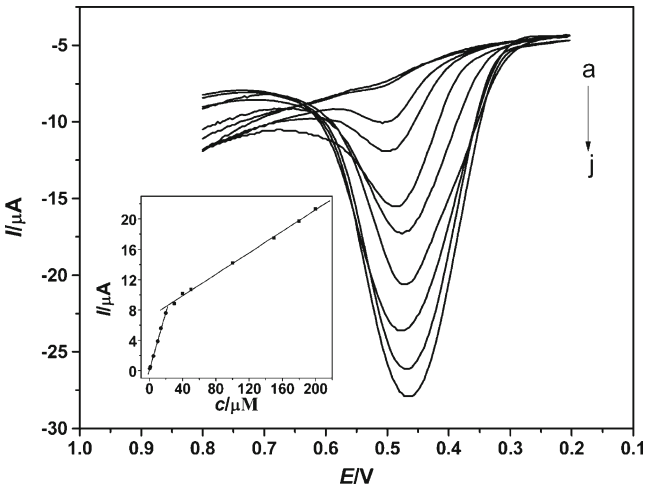

Fig. 6 DPV curves obtained in different concentrations (*a*→*j* 0.5, 1, 5, 10, 20, 40, 100, 150, 180, and 200 μM) of NP at FGNS^{IL}/GCE. *Insert* calibration curves

excellent sensitivity due to its electrocatalytic ability, huge surface, and excellent conductivity.

Reproducibility, stability, and interference

To investigate the reproducibility and stability of $FGNS^{IL}$/GCE, 50 μM NP solution was measured by ten modified GCE prepared independently with DPV. The relative standard deviation (RSD) was 3.33 %, showing that this method have good reproducibility. After the electrode was stored for 15 and 30 days at 4 °C in refrigerator, respectively, it could retain 94.3 and 91.6 % of its original response of 0.1 mM NP, which showed good stability of $FGNS^{IL}$/GCE.

The influence of some organics and inorganic ions on the detection of NP was investigated. The results suggested that 100-fold of Ni^{2+}, Co^{2+}, Fe^{3+}, Cu^{2+}, Ba^{2+}, K^{+}, Mg^{2+}, Al^{3+}, Zn^{2+}, Ca^{2+}, Cl^{-}, NO_3^{-}, HCO_3^{-}, CO_3^{2-}, Ac^{-}, hydroquinone, pyrocatechol, 2-nitrophenol, 2,4-dinitrophenol, 4-aminophenol, and 4-nitrophenol have no influence on the signal of 0.01 mM NP with peak current change below 5 % (see the supporting information), which indicated that $FGNS^{IL}$/GCE had a good selectivity to NP.

Analysis of NP in water and soil samples

To investigate the applicability of $FGNS^{IL}$/GCE, different kinds of real samples, tap water, Nai River water, and soil samples (collected from Tai'an, China) were used for quantitative analysis. Five grams of wet soil was dried in air and then extracted with 20 mL absolute ethanol for 1 h. Then, the solution was centrifuged. After filtration, the filtrate was collected in 25-mL volumetric flask and diluted to mark with absolute ethanol. One-milliliter sample solution was mixed with 9.0 mL PBS (pH=7.0). After accumulation for 350 s at −0.2 V, the analysis for oxidation peak of NP was measured by DPV. As no signals for NP was found in the samples, the concentration of NP was determined with standard addition methods. All the samples were investigated with three times at the same condition. As shown in Table 1, the average RSD was 3.10 %, which indicated good reproducibility. Moreover, the recoveries ranged from 94.8 to 104 %, illustrating $FGNS^{IL}$/GCE was able to analyze the NP in real samples.

Table 1 Determination of NP in local water and soil samples (n=3)

Samples	Added (μM)	Found (μM)	RSD (%)	Recovery (%)
Tap water	5.0	5.20	2.71	104.0
Nai river water	5.0	4.74	4.02	94.8
Soil	5.0	5.19	2.57	103.8

Interaction of NP with DNA

Figure 7 showed the relationship between $\log[\Delta I/\Delta I_{max}-\Delta I]$ and log[NP] in NP (10 to 50 μM) solutions containing different amounts of DNA. The insert graph was the DPV curves of 30 μM NP solutions in the absence (curve a) and presence (curve b) of 10 μg mL^{-1} DNA. The peak current decreased when DNA was added into the original solution due to the interaction between DNA and NP. Moreover, the oxidation peak potential shifted positively, which indicated that the binding of NP to DNA was via electrostatic interaction.

NP would be associated to a single complex $DNA{\cdot}NP_m$ with DNA according to previous report [43], and the reaction can be expressed as the following scheme:

$$DNA + mNP = DNA \cdot NP_m \quad (1)$$

The condition formation constant is as follows:

$$\beta^m = [DNA \cdot NP_m]/([DNA][NP]^m) \quad (2)$$

where β was the association constant, and m was Hill coefficient.

According to the overall Hill cooperativity model, the fraction of NP bond to DNA is given by:

$$f = [DNA \cdot NP_m]/\left([DNA \cdot NP_m]_{max}\right) = [DNA \cdot NP_m]/([DNA \cdot NP_m] + [DNA]) \quad (3)$$

where f was the fraction of NP binding sits filled, $[DNA{\cdot}NP_m]_{max}$ was the maximum concentration of $DNA{\cdot}NP_m$, $[DNA{\cdot}NP_m]$ represented the concentration of free $DNA{\cdot}NP_m$, and [DNA] was the concentration of free DNA.

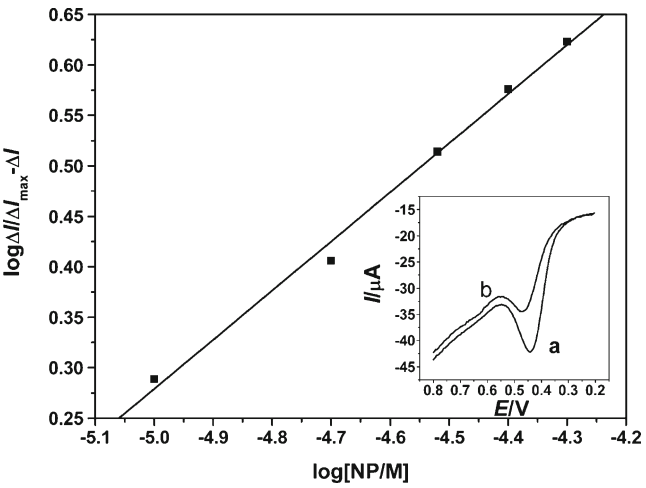

Fig. 7 The relationship between $\log[\Delta I/\Delta I_{max}-\Delta I]$ and log[NP] at $FGNS^{IL}$/GCE in 0.1 M PBS (pH=7.0). *Insert curves* the DPV curves in 30 mM NP (*a*) and 30 mM NP+10 μg mL^{-1} DNA (*b*)

The Hill coefficient was concluded from Eqs. (2) and (3):

$$\log[f/(1-f)] = m\log(\beta/\mathrm{M}^{-1}) + m\log([\mathrm{NP}]/\mathrm{M}) \quad (4)$$

and the following equations would be deduced:

$$[\mathrm{DNA}] = [\mathrm{DNA}]_0 - [\mathrm{DNA}\cdot\mathrm{NP}_m] \quad (5)$$

$$[\mathrm{NP}] = [\mathrm{NP}]_0 - m[\mathrm{DNA}\cdot\mathrm{NP}_m] \quad (6)$$

$$I = k[\mathrm{NP}] \quad (7)$$

$$\Delta I = k([\mathrm{NP}]_0 - [\mathrm{NP}]) = I_0 - I = k\times m\times[\mathrm{DNA}\cdot\mathrm{NP}_m] \quad (8)$$

$$\Delta I_{\max} = k\times m\times[\mathrm{DNA}\cdot\mathrm{NP}_m]_{\max} \quad (9)$$

From Eqs. (3), (8), and (9), the following equation was obtained:

$$f = \Delta I/\Delta I_{\max} \quad (10)$$

where $\Delta I_{\max}$ represents the maximum peak current value, which will be acquired when NP connected with DNA in the largest quantity.

Insert Eq. (10) into Eq. (3) to yield:

$$\log[\Delta I/\Delta I_{\max} - \Delta I] = m\log(\beta/\mathrm{M}^{-1}) + m\log([\mathrm{NP}]/\mathrm{M}) \quad (11)$$

If DNA and NP form a complex, then the plot of $\log[\Delta I/(\Delta I_{\max}-\Delta I)]$ versus log[NP] was linear with slope of m. As shown in Fig. 7, the linear relationship was concluded as $\log[\Delta I/(\Delta I_{\max}-\Delta I)]=2.712+0.487\log([\mathrm{NP}]/\mathrm{M})$ ($R=0.9966$). The Hill coefficient m was calculated as 0.4867, and the value of β was $3.75\times10^5\ \mathrm{M}^{-1}$. The result showed that DNA and NP formed a single complex.

Conclusion

In this paper, a reliable and sensitive electrochemical method was discussed for NP determination based on $\mathrm{FGNS^{IL}}$ modified electrode. The oxidation peak current of NP remarkably increased and the potential shift negatively under the optimum conditions at $\mathrm{FGNS^{IL}}$/GCE. The proposed method has been successfully applied in practical investigations of water and soil samples with good recoveries. The interaction between NP and DNA was also explored, and the result indicated that NP binding DNA formed a single complex. This fabricated electrode provided a new way for NP determination and the interaction of NP and DNA analysis.

Acknowledgments This work was supported by the National Natural Science Foundation of China (no. 21075078, 21105056) and the Natural Science Foundation of Shandong Province, China (ZR2010BM005, ZR2011BQ001).

References

1. Frassinetti S, Barberio C, Caltavuturo L, Fava F, Di Gioia D (2011) Genotoxicity of 4-nonylphenol and nonylphenol ethoxylate mixtures by the use of *Saccharomyces cerevisiae* D7 mutation assay and use of this text to evaluate the efficiency of biodegradation treatments. Ecotox Environ Safe 74:253–258
2. Soares A, Guieysse B, Jefferson B, Cartmell E, Lester J (2008) Nonylphenol in the environment: a critical review on occurrence, fate, toxicity and treatment in wastewaters. Environ Int 34:1033–1049
3. Z-y Wu, Z-d Z, Marriott PJ (2010) Comparative qualitative analysis of nonylphenol isomers by gas chromatography–mass spectrometry combined with chemometric resolution. J Chromatogr A 1217:7759–7766
4. Bärlocher F, Guenzel K, Sridhar KR, Duffy SJ (2011) Effects of 4-n-nonylphenol on aquatic hyphomycetes. Sci Total Environ 409:1651–1657
5. Spehar RL, Brooke LT, Markee TP, Kahl MD (2010) Comparative toxicity and bioconcentration of nonylphenol in freshwater organisms. Environ Toxicol Chem 29:2104–2111
6. Yang L, Lin L, Weng S, Feng Z, Luan T (2008) Sexually disrupting effects of nonylphenol and diethylstilbestrol on male silver carp (*Carassius auratus*) in aquatic microcosms. Ecotox Environ Safe 71:400–411
7. Bhattacharya H, Xiao Q, Lun L (2008) Toxicity studies of nonylphenol on rosy barb (*Puntius conchonious*): a biochemical and histopathological evaluation. Tissue Cell 40:243–249
8. Yao G, Ling L, Luan J, Ye D, Zhu P (2007) Nonylphenol induces apoptosis of Jurkat cells by a caspase-8 dependent mechanism. Int Immunopharmacol 7:444–453
9. Cox P, Drys G (2003) Directive 2003/53/EC of the European Parliament and of the council. Official Journal of the European Communities 17:2003
10. Loos R, Wollgast J, Castro-Jiménez J, Mariani G, Huber T, Locoro G, Hanke G, Umlauf G, Bidoglio G, Hohenblum P, Moche W, Weiss S, Schmid H, Leiendecker F, Ternes T, Ortega AN, Hildebrandt A, Barceló D, Lepom P, Dimitrova I, Nitcheva O, Polesello S, Valsecchi S, Boutrup S, Sortkjaer O, de Boer R, Staeb J (2008) Laboratory intercomparison study for the analysis of nonylphenol and octylphenol in river water. Trends Anal Chem 27:89–95
11. Bonenfant D, Niquette P, Mimeault M, Furtos-Matei A, Hausler R (2009) UV–VIS and FTIR spectroscopic analyses of inclusion complexes of nonylphenol and nonylphenol ethoxylate with [beta]-cyclodextrin. Water Res 43:3575–3581
12. Samsonova JV, Rubtsova MY, Franek M (2003) Determination of 4-n-nonylphenol in water by enzyme immunoassay. Anal Bioanal Chem 375:1017–1019
13. Lang W, Dejma C, Sirisansaneeyakul S, Sakairi N (2009) Biosorption of nonylphenol on dead biomass of *Rhizopus arrhizus* encapsulated in chitosan beads. Bioresource Technol 100:5616–5623
14. Cruceru I, Iancu V, Petre J, Badea I, Vladescu L (2011) HPLC-FLD determination of 4-nonylphenol and 4-*tert*-octylphenol in surface water samples. Environ Monit Assess. doi:10.1007/S10661-011-2151-2
15. Raecker T, Thiele B, Boehme RM, Guenther K (2011) Endocrine disrupting nonyl- and octylphenol in infant food in Germany: considerable daily intake of nonylphenol for babies. Chemosphere 82:1533–1540

16. MülazImoglu IE, MülazImoglu AD, Yilmaz E (2011) Determination of quantitative phenol in tap water samples as electrochemical using 3,3′-diaminobenzidine modified glassy carbon sensor electrode. Desalination 268:227–232
17. Geim AK (2009) Graphene: status and prospects. Science 324:1530–1534
18. Baby TT, Aravind S, Arockiadoss T, Rakhi R, Ramaprabhu S (2010) Metal decorated graphene nanosheets as immobilization matrix for amperometric glucose biosensor. Sensors and Actuators B: Chemical 145:71–77
19. Zhang Q, Qiao Y, Hao F, Zhang L, Wu S, Li Y, Li J, Song XM (2010) Fabrication of a biocompatible and conductive platform based on a single-stranded DNA/graphene nanocomposite for direct electrochemistry and electrocatalysis. Chemistry CA European Journal 16:8133–8139
20. Rao C, Sood A, Subrahmanyam K, Govindaraj A (2009) Graphene: the new two-dimensional nanomaterial. Angew Chem Int Edit 48:7752–7777
21. Chen D, Tang L, Li J (2010) Graphene-based materials in electrochemistry. Chem Soc Rev 39:3157–3180
22. Zhou M, Zhai Y, Dong S (2009) Electrochemical sensing and biosensing platform based on chemically reduced graphene oxide. Anal Chem 81:5603–5613
23. Shan C, Yang H, Song J, Han D, Ivaska A, Niu L (2009) Direct electrochemistry of glucose oxidase and biosensing for glucose based on graphene. Anal Chem 81:2378–2382
24. Fu C, Yang W, Chen X, Evans DG (2009) Direct electrochemistry of glucose oxidase on a graphite nanosheet-Nafion composite film modified electrode. Electrochem Commun 11:997–1000
25. Alwarappan S, Erdem A, Liu C, Li CZ (2009) Probing the electrochemical properties of graphene nanosheets for biosensing applications. J Phys Chem C 113:8853–8857
26. Wu S, Lan X, Cui L, Zhang L, Tao S, Wang H, Han M, Liu Z, Meng C (2011) Application of graphene for preconcentration and highly sensitive stripping voltammetric analysis of organophosphate pesticide. Anal Chim Acta 699:170–176
27. Parvin MH (2011) Graphene paste electrode for detection of chlorpromazine. Electrochem Commun 13:366–369
28. Yin H, Ma Q, Zhou Y, Ai S, Zhu L (2010) Electrochemical behavior and voltammetric determination of 4-aminophenol based on graphene-chitosan composite film modified glassy carbon electrode. Electrochim Acta 55:7102–7108
29. Yin H, Zhang Q, Zhou Y, Ma Q, liu T, Zhu L, Ai S (2011) Electrochemical behavior of catechol, resorcinol and hydroquinone at graphene–chitosan composite film modified glassy carbon electrode and their simultaneous determination in water samples. Electrochim Acta 56:2748–2753
30. Liu H, Liu Y, Li J (2010) Ionic liquids in surface electrochemistry. Phys Chem Chem Phys 12:1685–1697
31. Wei D, Ivaska A (2008) Applications of ionic liquids in electrochemical sensors. Anal Chim Acta 607:126–135
32. Safavi A, Maleki N, Farjami E, Mahyari FA (2009) Simultaneous electrochemical determination of glutathione and glutathione disulfide at a nanoscale copper hydroxide composite carbon ionic liquid electrode. Anal Chem 81:7538–7543
33. Liu Y, Li J, Wang M, Li Z, Liu H, He P, Yang X (2005) Preparation and properties of nanostructure anatase TiO_2 monoliths using 1-butyl-3-methylimidazolium tetrafluoroborate room-temperature ionic liquids as template solvents. Crystal growth & design 5:1643–1649
34. Zhang Q, Wu S, Zhang L, Lu J, Verproot F, Liu Y, Xing Z, Li J, Song X-M (2011) Fabrication of polymeric ionic liquid/graphene nanocomposite for glucose oxidase immobilization and direct electrochemistry. Biosens Bioelectron 26:2632–2637
35. Lu X, Zhang Q, Zhang L, Li J (2006) Direct electron transfer of horseradish peroxidase and its biosensor based on chitosan and room temperature ionic liquid. Electrochem Commun 8:874–878
36. Du M, Yang T, Ma S, Zhao C, Jiao K (2011) Ionic liquid-functionalized graphene as modifier for electrochemical and electrocatalytic improvement: comparison of different carbon electrodes. Anal Chim Acta 690:169–174
37. Shan C, Yang H, Han D, Zhang Q, Ivaska A, Niu L (2010) Electrochemical determination of NADH and ethanol based on ionic liquid-functionalized graphene. Biosens Bioelectron 25:1504–1508
38. Liu N, Luo F, Wu H, Liu Y, Zhang C, Chen J (2008) One-step ionic-liquid-assisted electrochemical synthesis of ionic-liquid-functionalized graphene sheets directly from graphite. Adv Funct Mater 18:1518–1525
39. Li Y, Wu Y (2009) Coassembly of graphene oxide and nanowires for large-area nanowire alignment. J Am Chem Soc 131:5851–5857
40. Luczak T (2008) Preparation and characterization of the dopamine film electrochemically deposited on a gold template and its applications for dopamine sensing in aqueous solution. Electrochim Acta 53:5725–5731
41. Usami M, Mitsunaga K, Ohno Y (2002) Estrogen receptor binding assay of chemicals with a surface plasmon resonance biosensor. J Steroid Biochem 81:47–55
42. Dempsey E, Diamond D, Collier A (2004) Development of a biosensor for endocrine disrupting compounds based on tyrosinase entrapped within a poly (thionine) film. Biosens Bioelectron 20:367–377
43. Qu F, Li NQ, Jiang YY (1998) Electrochemical studies of NiTM-pyP and interaction with DNA. Talanta 45:787–793